Eps8 involvement in neuregulin1-ErbB4 mediated migration in the neuronal progenitor cell line ST14A

Title: Eps8 involvement in neuregulin1-ErbB4 mediated migration in the neuronal progenitor cell line ST14A

Authors: Federica Fregnan[1], Veselin Petrov[1,6], Donatella Garzotto[1,7], Silvia De Marchis[1,5], Nina Offenhäuser[2] , Enrico Grosso[3,4], Giovanna Chiorino[3], Isabelle Perroteau[1,4,5] and Giovanna Gambarotta[1,4#]

1 Department of Animal and Human Biology, University of Turin - Italy

2 IFOM, The FIRC Institute for Molecular Oncology, Milan - Italy

3 Fondazione Edo ed Elvo Tempia Valenta, Cancer Genomics Laboratory, Biella - Italy

4 Center for Complex Systems in Molecular Biology and Medicine (SysBioM), University of Turin - Italy

5 Neuroscience Institute of Turin (NIT), Interdepartmental Centre of Advanced Studies in Neuroscience, University of Turin - Italy

6 present address: Department of Plant Physiology and Molecular Biology, University of Plovdiv - Bulgaria

7 present address: Dulbecco Telethon Institute, c/o Molecular Biotechnology Centre, University of Turin - Italy

Corresponding author with complete address, including an email address:

Giovanna Gambarotta

Department of Animal and Human Biology,

University of Turin,

Via Accademia Albertina, 13

10123 Turin - Italy

Tel.: +39-011-6704688, Fax: +39-011-6704508

e-mail: giovanna.gambarotta@unito.it

Keywords: Eps8, ErbB4, neuregulin1, migration, actin cytoskeleton, expression regulation

Abbreviations

ADAM 17, a disintegrin and metalloproteinase;

EGFR, epidermal growth factor receptor;

Eps8, epidermal growth factor receptor pathway substrate 8;

GO, gene ontology;

HGF/SF, hepatocyte growth factor/scatter factor;

NRG1, neuregulin 1;

OB, olfactory bulb;

PI3K, phosphatidylinositol 3-kinase;

qRT-PCR, quantitative real time RT-PCR;

RMS, rostral migratory stream;

SVZ, subventricular zone;

TACE, tumor-necrosis-factor-α-converting enzyme.

Abstract

Stable expression of the tyrosine kinase receptor ErbB4 confers increased migratory behavior to the neuronal progenitor cell line ST14A, in response to neuregulin 1 (NRG1) stimulation. We used gene expression profiling analysis to identify transcriptional changes associated with higher migratory activity caused by the activation of a specific ErbB4 isoform, and found constitutive up-regulation of the Epidermal growth factor receptor pathway substrate 8 (Eps8), a multimodular regulator of actin dynamics.

We confirmed the increase of Eps8, both at the mRNA and at the protein level, in stable clones expressing two different ErbB4 isoforms, both characterized by high migratory activity.

Using Transwell assays and experimental manipulation of Eps8 expression level, we demonstrated that Eps8 synergizes with ErbB4 to increase both basal and ligand induced cell migration, whereas siRNA mediated Eps8 silencing strongly impairs cell motility and NRG1 induced actin cytoskeleton remodeling.

By transient knockdown of Eps8 through *in vivo* siRNA electroporation, followed by explant primary cultures, we demonstrated that Eps8 down-regulation affects migration of normal neuronal precursors.

In conclusion, our data demonstrate that Eps8 is a key regulator of motility of neuronal progenitor cells expressing ErbB4, both in basal conditions and in response to external motogenic cues.

Introduction

ErbB4 is a tyrosine kinase receptor belonging to the Epidermal growth factor receptor (EGFR/ErbB1) family, involved in regulating neuronal migration [1-3]. This protein, like the other members of the EGFR family, can form homo- and hetero-dimers and presents an extracellular domain for interaction with the ligands, a single transmembrane region and a cytoplasmic domain that possesses tyrosine kinase activity [4]. The ErbB4 gene is characterized by two alternative splicing, producing four different isoforms. One isoform pair is characterized by alternative splicing of exons located in the extracellular juxtamembrane region, conferring susceptibility (JMa) or not (JMb) to proteolytic cleavage [5] by the metalloproteinase TACE ("tumor-necrosis-factor-α-converting enzyme") also known as ADAM 17 ("a disintegrin and metalloproteinase"). ErbB4 ectodomain shedding triggers a second presenilin-dependent γ-secretase cleavage, which releases from the membrane a cytoplasmic ErbB4 domain, that translocates into the nucleus and regulates transcription [6-13]. The other ErbB4 isoform pair is characterized by the presence (cyt1) or absence (cyt2) of a cytoplasmic exon containing a docking site for phosphatidylinositol 3-kinase (PI3K) [14, 15] and for WW-domain containing ubiquitin ligases involved in ubiquitination and degradation of the receptor [16-19].

Two of the four ErbB4 isoforms (JMa-cyt2 and JMb-cyt1) confer, upon neuregulin 1 (NRG1) stimulation, a high migratory activity to the neuronal progenitor cell line ST14A [20, 21].

We show here that in stable ST14A clones expressing these two ErbB4 isoforms, Eps8 ("EGFR pathway substrate 8") mRNA and protein are up-regulated. Eps8 has been identified among proteins phosphorylated on tyrosine following EGFR activation [22]; Eps8 exists in two isoforms, of 97- and 68-kDa [22], and is involved in regulation of actin dynamics. The actin cytoskeleton participates in many cellular processes including regulation of cell shape, motility and adhesion. Remodeling of the actin cytoskeleton is dependent on actin binding proteins, which organize actin filaments into specific structures that allow them to perform specialized

functions. Eps8 is involved in actin regulation in at least three different ways: 1) forming a complex with Abi1, p85 (the regulatory subunit of phosphatidylinositol-3-kinase, PI3K) and the guanine exchange factor Sos-1, promoting the activation of Rac [23]; 2) capping the barbed-end of actin [24] and 3) bundling actin filaments [25].

In this study we analyzed the involvement of Eps8 in the ErbB4 mediated migration in a cellular model of neuronal progenitors.

Material and methods

Cell Cultures and Reagents - All chemicals and reagents were purchased from Sigma (St. Louis, MO), unless otherwise stated. The ST14A cell line (kindly provided by prof. Elena Cattaneo) was derived from primary cells dissociated from embryonic day 14 rat striatal primordia as previously described [20]. Cells were cultured on dishes (BD Biosciences, San Jose, CA, USA) in Dulbecco's modified Eagle's medium (DMEM) containing 4.5 g/l glucose, 1 mM sodium pyruvate, 2 mM L-glutamine and supplemented with 100 units/ml penicillin, 0.1 mg/ml streptomycin and 10% fetal bovine serum (FBS, Gibco®, Carlsbad, CA, USA) inactivated for 30 min at 56°C (or 2% FBS or serum free medium for starvation before assays, as described below). Stable transfectants were grown in medium containing 5 µg/ml puromycin. Cells were grown as monolayers at the permissive temperature of 33°C in a 5% CO_2 atmosphere saturated with H_2O. Cells were allowed to grow to near-confluence, and adherent cells were harvested by the trypsin/EDTA method. For ligand stimulation experiments, 12.5 ng/ml hepatocyte growth factor/scatter factor (HGF/SF, Sigma) or 5 nM recombinant NRG1β1 (henceforth called NRG1) were used; the EGF-like domain of mouse NRG1 has been produced in the laboratory as a His-tag fusion protein in *E.coli* [26]. For experiments with PI3 kinase or γ-secretase inhibitors, stable clones B1.15 and A2.1 were grown in 10% FBS DMEM until 60% confluence. Then the serum was lowered to 2% and cells were treated for 24, 48, 72, 96 hours with 10 µM LY294002 (Calbiochem), for 22, 48, 72 hours with 10 µM DAPT (γ-secretase inhibitor compound IX, Calbiochem). As a mock control, cells were treated with an equal volume of solvent (DMSO). The medium containing inhibitors or DMSO was replaced every 48 hours.

RNA extraction from ST14A cells - Total RNA was prepared using the TRIzol reagent (Invitrogen, Carlsbad, CA, USA) according to the manufacturer's instructions.

Microarray - We first optimized the conditions for a migratory response: starting from the

standard Transwell assay conditions (2% serum, 5 nM NRG1, 18 hours) we performed time course experiments to determine the optimal stimulation time and growth conditions. We could detect a specific migratory response to NRG1 already after 12 hours of stimulation and we hypothesized that transcriptional regulation of effectors involved in the regulation of cell migration would be detectable after this time interval. RNA was extracted from NRG1 stimulated stable clone A2.12 and mock ST14A cells. Total RNA was amplified and labeled using Ambion Message Amp I. Cy3- and Cy5-labeled RNAs were hybridized with a dye-swap replication scheme on Whole Rat Genome Microarray (Agilent Technologies, Santa Clara, CA, USA) containing 41000 unique probes that represent 21337 well-known rat genes and transcripts, including homologues to human and mouse genes. Arrays were scanned with the Agilent B scanner and image files were loaded into Feature Extraction software version 7.6 (Agilent Technologies) to obtain raw data. Raw data files were then loaded onto the Resolver SE System (Rosetta Biosoftware, Seattle, WA, USA) to perform data processing and normalization using the platform-specific error model. The two replicated ratio profiles were combined, associating each gene to an expression fold-change and a p-value to assess the statistical significance of its modulation in the A2.12 ST14A sample compared with the mock one, both following stimulation with 5 nM NRG1 for 12 hrs. RNA quality was checked by Agilent 2100 Bioanalyzer (Agilent Technologies). Concentrations and labeling were also checked by NanoDrop ND-1000 Spectrophotometer (Thermo Fisher Scientific, Wilmington, DE, USA).

Microarray data analysis - A gene ontology (GO) enrichment analysis with Database for Annotation, Visualization and Integrated Discovery software (DAVID, http://david.abcc.ncifcrf.gov/) was performed to identify enrichment clusters in which highly related genes are bunched in functional related groups. 143 clusters of related genes were identified. We focused our attention on clusters involved in cell motility, actin cytoskeleton

organization, cell adhesion and generated heatmaps from these clusters. Three representative clusters and the corresponding heatmaps are shown in figures S1 and S2. Four candidate genes, possibly involved in cell migration, were chosen (Cxcl12/SDF-1, Eps8, tymosin beta like, mesothelin). An additional analysis with Kegg software (http://www.genome.jp/kegg/pathway.html, not shown) allowed us to choose other 4 candidate genes (FGF5, stathmin-like 4, kelch-like 13, MMP24). With Metacore database and software, all regulated genes were analysed to obtain networks of interacting proteins; in figure S3 is shown a representative network containing ErbB4 and some regulated genes involved in cell migration. The list of the eight candidate genes analyzed by qRT-PCR is shown in table S2.

Reverse transcriptase (RT) -Total RNA was diluted to 0.2 µg/µl and 5 µl (1 µg) were subjected to a reverse transcriptase reaction in 25 µl reaction volume containing: 1X RT-Buffer (Fermentas, Burlington, Canada); 0.1 µg/µl bovine serum albumin (BSA, Sigma); 0.05% Triton X-100; 1 mM dNTPs; 7.5 µM random exanucleotide primers (Fermentas); 1 U/µl RIBOlock (Fermentas) and 200 U RevertAid™ M-MuLV reverse transcriptase (Fermentas). The reaction was performed for 10 min at 25°C, 90 min at 42°C, 10 min at 90°C. For each sample, also a reaction in the absence of the enzyme was performed (RT-) and analyzed by PCR.

Quantitative real-time RT-PCR analysis – The system used for qRT-PCR analysis was ABI Prism 7300 (Applied Biosystems). To check for DNA contamination, a control RT reaction was set up for each sample without the addition of reverse transcriptase. cDNA was diluted 10 times before analyses and 5 µl were analysed in a total volume of 25 µl containing 1X PowerGREEN Master Mix (Applied Biosystems), and 300 nM of each primer. The reactions were carried out in 40 cycles (primer annealing temperature: 60°C). For each cDNA sample, a

technical triplicate was made and dissociation curves were routinely performed to check for the presence of a single peak corresponding to the required amplicon. Normalized reporter fluorescence *(Rn)* for each cycle was obtained by normalizing SYBRGreen to ROX signal. To normalize, we didn't follow the classic ΔΔCT method, which assumes 100% primer efficiency and uses a single reference gene for normalization. Primer efficiency and cycle threshold (CT) were calculated by means of the Miner software (www.miner.ewindup.info/miner), accordingly to an algorithm [27], which fits a logistic curve on the experimental plot and uses the noise level of the entire curve to determine the beginning of the exponential phase and the second derivative maximum to determine its end. To normalize, we used the geometric average of two reference genes, Ubiquitin C (UbC) and TATA box binding protein (TBP) [28]. The normalized relative quantity was calculated accordingly to a formula which takes into account the variations in primer efficiency among different assays and can deal with multiple reference genes [29, 30].

Primers were designed using Primer Express 1.5 software (Applied Biosystems), checked with Annhyb software (http://www.bioinformatics.org/annhyb/) and synthesized by Sigma-Genosys.

The expression of eight candidate genes (table S2) identified by microarray analysis was quantified by qRT-PCR. The sequences of the primers for Eps8 (XM_232499.4) are: 5'-CCTCCCCGGAAGAAGTGAAG-3' (forward) and 5'-AAAAGAGTTGCGCTCCGTTC-3' (reverse); for the housekeeping gene UbC (NM_017314) are: 5'-TCGTACCTTTCTCACCACAGTATCTAG-3' (forward), and 5'-GAAAACTAAGACACCTCCCCATCA-3' (reverse); for the housekeeping gene TBP (NM_001004198) are: 5'-TAAGGCTGGAAGGCCTTGTG-3' (forward) and 5'-TCCAGGAAATAATTCTGGCTCATAG-3' (reverse). The sequences of the other primer pairs are available on request.

siRNA and DNA transfection - siRNA transfection was performed with 3 different anti-rat Eps8

siRNAs (EPS8_PREDICTEDRSS319884, EPS8_PREDICTEDRSS319885, EPS8_PREDICTEDRSS319886, Invitrogen, Life Technologies Corporation, Carlsbad, California, USA) hereafter marked as #84, #85 and #86. Scramble siRNA (Stealth™ RNAi Negative control medium GC duplex, Invitrogen) was used as a control. The Lipofectamine 2000 (Invitrogen) reagent was used to drive transfection of 10 nM siRNA in Opti-MEM medium (Gibco®) according to manufacturers' instructions; we favored 10nM siRNA concentration, because we observed an unspecific inhibition of migration in cells treated with 20 nM scramble siRNA.

For transient transfection of plasmidic DNA, 3 µg of each construct (or the empty vector as a mock control) were transfected in a 6 cm diameter dish, using 1 µl Lipofectamine 2000/µg DNA, according to manufacturers' instructions. The Transwell assays were performed 48 hrs after siRNA or DNA transfection; total proteins were extracted from leftovers of the transfected cells to check, by western blot analysis, for siRNA activity and Eps8 down-regulation, or for transient overexpression of candidate proteins (ErbB4, Eps8). For DNA transient transfection, the expression vectors pIRESpuro2-ratErbB4-JMb-cyt1, pIRESpuro2-ratErbB4-JMa-cyt2 [21], pCEV-mouseEps8 [31], actin M-cherry (prof. Kenneth Yamada, NIH/NIDCR) were used.

Transwell assays – Transwell assays were performed as previously described [21]. Four images were analyzed for each Transwell and the amount of migrated cells was evaluated as the total area of migration (in pixel^2) calculated with the Image J software and then expressed as percentage of the total number of migrated cells for every single experiment. Cells were discriminated by the pores of the Transwell membrane by applying a threshold of 300 pixel^2. For every experimental condition a technical triplicate was made and each experiment was repeated 3 times to obtain data as a biological triplicate.

Total protein extraction, and western blot - Total proteins were extracted by solubilizing cells in boiling Laemmli buffer (2.5% SDS and 0.125 M Tris-HCl pH 6.8), followed by 3 min at 100°C. For the time course experiments, cells were rinsed twice with ice-cold PBS containing 1 mM sodium orthovanadate and lysed for 20 min on ice with 500 µl cold extraction buffer (20 mM Tris-HCl (pH 7.4), 150 mM NaCl, 5 mM EDTA, 2 mM EGTA, 1 mM $ZnCl_2$, 50 mM NaF, 10% glycerol, and 1% Triton X-100 supplemented just prior to use with 1 mM sodium orthovanadate, 1 mM phenylmethylsulfonyl fluoride, and a mixture of protease inhibitors (Roche Applied Science). Lysates were collected with a cell scraper, placed in microcentrifuge tubes, rocked at 4 °C for 10 min, and spun at 4 °C for 20 min at 11,000 g to discard cell debris. Protein concentration was determined by the BCA method, and equal amounts of proteins (denaturated at 100°C in 240 mM 2-mercaptoethanol and 18% glycerol) were loaded onto each lane, separated by SDS-PAGE, transferred to a HybondTM C Extra membrane, and analyzed as previously described [21]. Conclusions were drawn after experiments were repeated a minimum of three times. Primary antibodies used are: rabbit polyclonal anti-ErbB4 (1:500, sc-283, Santa Cruz Biotechnology, Santa Cruz, CA, USA); rabbit polyclonal anti-ErbB2 (1:500, sc-284, Santa Cruz Biotechnology); rabbit polyclonal anti-ErbB3 (1:500, sc-285, Santa Cruz Biotechnology); mouse monoclonal anti-Eps8 (1:1000, #610143, BD Transduction Laboratories); rabbit monoclonal anti-phospho-ErbB4 (Tyr1284) (1:500, #4757, Cell Signaling Technology); mouse monoclonal anti-actin (1:4000, #A5316, Sigma); horseradish peroxidase-linked donkey anti-rabbit secondary antibody (Amersham Biosciences) was used at 1:10.000 dilution, sheep anti-mouse secondary antibody (Amersham Biosciences) was used at 1:10.000 to detect Eps8, 1:100.000 to detect actin.

Actin remodeling assay- Subconfluent A2.1 cells (in a 6 cm diameter plate) were transiently co-transfected with 10nM siRNAs (control or #85-#86 pool, see above) and 1 µg plasmidic DNA coding for actin-M cherry (kindly provided by Kenneth Yamada, NIH/NIDCR) with

Lipofectamine 2000, as described above. The following day, cells were plated in a 12 well plate containing poly-lysine pretreated coverslips. Three hours later cells were washed with PBS and serum starved for 24 hours. Then, 5 nM NRG1 was added to the cells and 6 hours later treated and untreated cells were fixed in 4% paraformaldehyde (PFA) for 20 minutes. Coverslips were mounted using a DABCO-based antifade mounting medium.

All images were captured with a Nikon DS Camera Head (DS-Fi1/DS-5M/DS-2Mu/DS-2MBW), equipped with DS Camera Control Unit DS-L2, connected to a Nikon inverted fluorescence microscope Eclipse-Ti-S. For each experimental condition, three independent samples were examined for actin organization; the entire procedure was carried out in a blind manner. For each sample, 25-30 microscopic fields (objective 40x) were analyzed, in order to score 100-110 cells.

RNA and protein extraction from mouse tissue microdissections - Total RNA and proteins were extracted from microdissection samples using the TRIzol reagent (Invitrogen, Carlsbad, CA, USA) according to the manufacturer's instructions. To obtain microdissection samples, CD1 mice from postnatal day 5 (P5) were anesthetized by hypothermia and then rapidly decapitated. Brains were dissected out and placed in ice-cold Leibovitz-15 medium (L-15) (Invitrogen) before embedding. Brains embedded in 3% low-melting point agar in L-15 were vibratome cut (Leica VT100S, Wetlzar, Germany) into 250 µm thick coronal slices in L-15 medium. Tissues from SVZ, posterior RMS, anterior RMS and surrounding OB were isolated under a high magnification dissecting microscope (Leica) and trimmed into pieces, which have been frozen for the following RNA and protein extraction with Trizol reagent (Invitrogen). To isolate the entire OB, adult mice were deeply anesthetized with a mixture of Ketamine : Xilazine (4 : 1).

In vivo electroporation procedure, SVZ explant cultures, neuroblast migration analysis - For *in vivo* electroporation assays, we used as a negative control a scramble 488 Alexa Fluor labelled siRNA (Stealth™ RNAi Negative control medium GC duplex, Invitrogen, the same sequence used for *in vitro* assays), while to down-regulate Eps8, we utilized a 555 Alexa Fluor labelled Stealth™ siRNA; Eps8 sequence, corresponded to the EPS8_PREDICTEDRSS319886 siRNA (#86, here used for *in vitro* assays), with a changed nucleotide to obtain perfect match with mouse Eps8 sequence (the silencing efficiency of #85 and #86 siRNAs in rat is the same; we chose to modify the #86 siRNA to electroporate mice, because its sequence is more similar to the corresponding mouse Eps8 sequence). The Alexa Fluor labelled siRNA efficiency has been verified by western blot (figure 8C).

For the electroporation procedure, we followed the protocol for DNA described by Camille Boutin [32], with some adaptations. One to three days old pups (P1-P3; CD1 strain mice, Charles River, Calco, Italy) were anesthetised by hypothermia (4 min) and immobilized on a custom neonatal stereotaxic apparatus maintained at 4°C during surgery. The skull was exposed by a skin incision and 1µl of 50µM 488/555 AlexaFluor labelled siRNA (Invitrogen) in PBS solution was injected into the right lateral ventricle at stereotaxic coordinates of 0 mm bregma, 1 mm lateral to sagittal sinus, and 2 mm depth, by means of a glass micropipette and a pneumatic pressure injection apparatus (Picospritzer II; General Valve, Fairfield, IL). After the micropipette was removed, the skin was sutured with 0.8 mm silk thread. Injected animals were subjected to two series of five electrical pulses (99,9 volts, 50 ms, separated by 950 ms intervals) using the CUY21SC device (Nepagene, Chiba, Japan) and 5 mm tweezer electrodes (CUY650P5, Nepagene) rinsed in PBS before each electroporation. Electroporated animals were reanimated for several minutes under a heating lamp before being returned to the dam.

Tissue explant cultures were obtained 48 hrs after electroporation, as previously described [33]. Briefly, mice were anesthetized by hypothermia and then killed by rapid decapitation.

Brains were dissected out and placed in ice-cold Leibovitz-15 medium (L-15), (Invitrogen); the right electroporated hemispheres were embedded in 3% low-melting point agar in L-15 and vibratome (Leica VT100S) cut into 250-µm-thick coronal slices in ice-cold L-15 medium. Tissues from SVZ lateral ventricle presenting fluorescent cells were isolated under a high magnification dissecting microscope (Leica) and trimmed into pieces of ~250 µm. Explants were subsequently embedded in 20% Neurobasal medium (NB) (Invitrogen)-80% Matrigel (BD Biosciences). Explants were maintained 2 days *in vitro* (2 DIV) in 5% CO2 at 37°C in NB medium supplemented with 1 x B27 (Invitrogen), 25 µg/ml gentamicin (Invitrogen), and 0.5 mM glutamine (Invitrogen). For analysis, tissue explants were fixed in 4% paraformaldehyde (PFA) for 40 min and stained with the nuclear marker DAPI (Molecular Probes) for 30 min at room temperature. Some explants were processed for western blot analysis to verify the siRNA effect. All tissue explant images were captured with a Leica DC500 photocamera (Leica Microsystems AG) connected to an Olympus 1X51 fluorescence microscope. Quantification of cell migration from the explants was performed on DAPI labelled specimens. The migration area was evaluated on digitalized images as the surface covered by DAPI nuclear staining, excluding the tissue explant area by means of Image J software [33]. The procedure has been carried out in a blind manner.

Statistical analyses – Whenever results are presented in excel graphs, at least three independent experiments (biological triplicate) were carried out in a technical triplicate. Data are presented as mean + standard error of the mean, SEM. Data were analyzed by SPSS software, One-Way ANOVA and post hoc analysis by means of Bonferroni test. Transwell migration assay data were assessed by Friedman test and Bonferroni post hoc analysis.

Results

Microarray analysis of regulated genes following ErbB4 receptor stimulation

We previously generated and characterized stable clones of the rat neuronal progenitor cell line ST14A [20], each expressing only one of the four different ErbB4 isoforms (fig. 1B), which confer different migratory capabilities in response to the ligand NRG1 [21]. To better understand the molecular mechanisms involved in ErbB4-mediated migration, we thought to identify genes which are regulated in this process. We chose a stable clone expressing the JMa-cyt2 ErbB4 isoform (which confers high migratory activity) and a pool of mock transfected cells as a control. We prepared mRNA from NRG1 stimulated cells, and performed a comparative analysis using oligo glass arrays. The total number of genes modulated above 2-fold and with p-value less than 10^{-7} was 642, of these 377 genes were down-regulated and 265 were up-regulated (see table S1).

Eps8 over-expression correlates with ErbB4 mediated migration activity in the rat neuronal progenitor cell line ST14A

We submitted the list of regulated genes to a functional analysis by means of the Database for Annotation, Visualization and Integrated Discovery software (DAVID, http://david.abcc.ncifcrf.gov/) which enables the discovery of biological themes within gene lists and the generation of gene annotation tables (see microarray data analysis in material and methods and figs. S1 and S2). We performed further analyses with the Kegg pathways database (http://www.genome.jp/kegg/pathway.html, data not shown) and Metacore (fig. S3), to define a list of candidate genes, potentially implicated in cell migration.

By quantitative real time RT-PCR (qRT-PCR, data not shown) we evaluated the expression of eight candidate genes (table S2) in the stable clone expressing the JMa-cyt2 ErbB4 isoform. Six of the eight genes are regulated according to the microarray data. Next, we tested the regulation of these genes in our experimental system in which expression of different ErbB4

isoforms confers different migratory ability to the cells. We considered two independent clones for each ErbB4 isoform, in order to eliminate clonal variations and a pool of mock transfected cells was used as control. We focused our attention on Eps8, the only gene whose expression pattern among clones expressing the different ErbB4 isoforms (fig. 1A) matches the clone tendency to migrate following NRG1 stimulation (fig. 1B). Eps8 is a multimodular regulator of actin dynamics, belonging to functional classification clusters associated to cell motility and to the same interaction network of ErbB4 (figs. S1-S3).

We found that the level of Eps8 mRNA is significantly higher in highly migrating clones expressing JMb-cyt1 and JMa-cyt2 ErbB4 isoforms, and lower in slowly migrating clones, expressing JMa-cyt1 and JMb-cyt2 ErbB4 isoforms. In addition, mock cells that do not express ErbB4 and do not migrate when stimulated with NRG1, present the lowest amount of Eps8 transcript. This observation was also confirmed at the protein level (fig. 2), where we observed a direct correlation between the Eps8 expression level and the migratory behavior of the cells, but not between Eps8 and ErbB4 expression levels: A1, B1 and B2 clones produce almost the same amount of ErbB4, but only B1 clones display very abundant Eps8 protein level.

Two Eps8 isoforms (likely derived by alternative splicing) were described: a full length 97 kDa and a truncated 68 kDa one [22]. Stable cell clones expressing different ErbB4 isoforms exhibit the two Eps8 isoforms with different intensity: JMb-cyt1 clones show a higher expression of the 97 kDa isoform, whereas for JMa-cyt2 clones the ratio between expression of 97 and 68 kDa is lower.

Eps8 expression is down-regulated by PI3K inhibitor treatment in JMb-cyt1 expressing cells and by γ-secretase inhibitor treatment in JMa-cyt2 expressing cells.

The two ErbB4 isoforms expressed by stable clones characterized with a high migratory activity and Eps8 up-regulation, differ in many aspects: ErbB4 JMb-cyt1 does not release

extracellular or intracellular fragments, but can directly activate PI3K and is internalized and degraded more efficiently than ErbB4 JMa-cyt2. Cells expressing this ErbB4 isoform display the highest Eps8 level, not further up-regulated by ligand treatment.

ErbB4 JMa-cyt2 releases an extracellular domain and a cytoplasmic fragment which can translocate into the nucleus and influence gene transcription. Cells expressing this ErbB4 isoform express Eps8 protein, which is further up-regulated following ligand stimulation.

We hypothesized that the JMa-cyt2 isoform activates Eps8 transcription through the release of the intracellular fragment, whose nuclear localization increases following NRG1 stimulation [11], the JMb-cyt1 isoform through the PI3K activation. According to this model, the isoform JMa-cyt1, which releases an intracellular fragment, does not increase Eps8 expression, because the intracellular fragment is rapidly degraded and does not translocate into the nucleus; the JMb-cyt2 isoform, does not increase Eps8 expression, because it does not activate directly the PI3 kinase pathway.

To test these hypotheses, we performed time course experiments treating both JMb-cyt1 and JMa-cyt2 expressing cells with the γ-secretase inhibitor DAPT (which inhibits the release of the intracellular fragment), or with the PI3-kinase inhibitor LY294002, or with the solvent (DMSO) as a control. We demonstrated that Eps8 protein expression decreases 96 hours after LY294002 treatment in cells expressing the JMb-cyt1 isoform (fig. 3, upper panel) and 72 hours after DAPT treatment in cells expressing the JMa-cyt2 isoform (fig. 3, lower panels). The expression of ErbB2 and ErbB3 receptors, in addition to the actin, was analyzed to exclude non-specific effects of chemical inhibitors on protein expression.

These results suggest that JMa-cyt2 and JMb-cyt1 activate Eps8 transcription via independent and different mechanisms.

NRG1 treatment stimulates Eps8 up-regulation in ST14A cells stably expressing JMa-cyt2 ErbB4

To investigate whether NRG1 treatment regulates Eps8 expression at the protein level, we performed a time course assay in the time window comprised between 0 and 120 minutes following NRG1 stimulation of serum starved cells.

Cells expressing JMb-cyt1 isoform (clone B1.15) show a high basal level of Eps8 which does not further increase following NRG1 stimulation (fig. 4A). JMa-cyt2 isoform expressing cells (clone A2.1) display a lower level of the Eps8 protein which increases 45 minutes after NRG1 stimulation (fig. 4B).

These data are in accord with the Eps8 transcript relative quantification (fig. 1A) which shows that NRG1 treatment stimulates Eps8 transcription in the stable clone A2.1 and that B1 stable clones express more Eps8 than A2 stable clones.

In a longer time course assay we observed that Eps8 up-regulation persists for 18 hours following NRG1 stimulation (fig. 4C).

ErbB4 and Eps8 transient co-expression confers to ST14A cells the ability to migrate

Our data show that ST14A clones stably expressing ErbB4 JMb-cyt1 or JMa-cyt2, are characterized by high levels of Eps8 and elevated migratory activity. To understand if ErbB4 and Eps8 expression are necessary and/or sufficient to confer higher migratory ability following NRG1 stimulation, we transiently transfected the mock pool of ST14A cells with expression vectors for ErbB4 (isoform JMb-cyt1), Eps8 or both. We observed that, while transient Eps8 expression does not change the migratory ability of the cells, transient expression of ErbB4 provokes an augmentation in cell migration. ErbB4 and Eps8 co-expression further increases both NRG1 induced and basal migration, suggesting that ErbB4 and Eps8 regulate migratory activity synergistically (fig. 5). The transient transfection of the JMa-cyt2 isoform produced the same results (data not shown). No Eps8 up-regulation was

observed in cells transiently transfected with only ErbB4 (data not shown); this suggests that the time window of the transient transfection (48-72 hours) is not sufficient to activate Eps8 transcription.

Eps8 down-regulation inhibits migration in ST14A cells expressing ErbB4

To investigate the role of Eps8 in NRG1 induced migration, a subtractive approach was chosen by means of RNA interference. To achieve an effective down-regulation of Eps8, various transfection conditions were tried, testing three different siRNAs at different times and concentrations (figs. 6A and 6B). While all the three tested siRNAs efficiently down-regulate the 97 kDa variant of Eps8, only siRNAs #85 and #86 turn off effectively also the 68 kDa isoform. To distinguish the effects of knocking down both Eps8 isoforms or only the 97 kDa one, all assays were carried out with a pool of #85-#86 siRNAs (figs. 6B and 6C) to down-regulate both Eps8 isoforms, #84 siRNA to down-regulate only the 97 kDa isoform and scramble siRNA (CTR) as a negative control.

Transwell assays were performed with cells transiently transfected with siRNAs in the temporal window extending between 48 and 66 hours after transfection. Two representative stable clones were chosen for this assay, expressing a high Eps8 level and the ErbB4 isoform JMb-cyt1 (clone B1.15) or JMa-cyt2 (clone A2.1).

As shown in figures 6D and 6E, the transient expression of siRNAs directed versus Eps8 impairs the NRG1 induced migratory activity of cells expressing either JMb-cyt1, or JMa-cyt2 ErbB4 isoform. Statistical analysis demonstrates that down-regulation of Eps8 97 kDa isoform is sufficient to inhibit ligand stimulated migratory activity. Moreover, in non stimulated B1.15 cells (grown in 2% FBS medium) basal migration is decreased after treatment with anti-Eps8 #85-86 siRNAs.

To investigate whether Eps8 plays a more general role in migration, we treated Eps8 siRNA transfected cells with hepatocyte growth factor/scatter factor (HGF/SF), a growth factor known

to induce c-Met mediated migration [34, 35]. We observed that Eps8 down-regulation inhibits HGF/SF induced migration (data not shown), demonstrating that in our cell model Eps8 silencing interferes with migration regulated by different receptor tyrosine kinases.

NRG1 induces reorganization of actin cytoskeleton, which is reduced by Eps8 silencing

It has been previously demonstrated that in ST14A cells 6 hours HGF/SF treatment triggers reorganization of the actin cytoskeleton [34, 35]. To visualize the actin cytoskeleton in ErbB4 expressing ST14A cells, we transiently transfected an expression vector for actin M-cherry fluorescent protein. The expression of this protein doesn't interfere with actin remodeling, as assessed by previous preliminary experiments. Serum starved cells were treated with NRG1 for 6 hours and quantitatively analyzed for actin cytoskeleton organization (fig. 7). Fluorescent actin in control starved cultures showed a diffuse network of stress fibers in a high cell percentage; we observed that, following NRG1 treatment, the percentage of cells showing organized actin is significantly reduced and actin is accumulated in lamellipodia.

To test the involvement of Eps8 in actin cytoskeleton reorganization, the same experiment was performed by transiently co-transfecting actin M-cherry and the pool of #85-#86 siRNAs directed versus Eps8 (or scramble siRNA as a control).

When Eps8 is transiently down-regulated by siRNA treatment, there is a reduction in stress fiber formation upon starvation and the percentage of cells showing organized actin is not significantly different when comparing NRG1 stimulated and not-stimulated cells (fig. 7), suggesting that Eps8 down-regulation interferes with actin cytoskeleton organization and dynamics.

Transient Eps8 down-regulation inhibits migration of neuronal precursors expressing ErbB4 and Eps8

To determine whether endogenous Eps8 regulates migration of normal neuronal precursor

cells expressing ErbB4, we focused our attention on neuronal progenitors which, during development and in adult life, originate in the subventricular zone (SVZ), migrate tangentially in chains through the rostral migratory stream (RMS) and reach the olfactory bulb (OB), where they eventually differentiate into granule and glomerular interneurons. It has been already demonstrated that these neurons express NRG1 and ErbB4 [36]; we demonstrate here that Eps8 protein is expressed in the SVZ, in the RMS, in the OB (figs. 8A and 8B), and that the four ErbB4 isoforms are expressed in the same regions (data not shown).

siRNAs directed against Eps8 (or scramble control siRNAs) were injected into the lateral ventricle of P1-P3 mice and *in vivo* electroporated. Forty-eight hours later, animals were sacrificed and explants of the SVZ region were cultured in Matrigel *in vitro* for 48 hours. In order to analyse migration in conditions as “physiological” as possible, exogenous soluble ligand was not added, since it is already produced by migrating neuroblasts [36]. Efficient down-regulation of Eps8 was verified by western blotting on explant total protein extracts (fig. 8C). When SVZ explants are cultured, compact chains of polysialylated neural cell adhesion molecule-positive (PSA-N-CAM+) migrating neuroblasts are symmetrically distributed around the explant, whereas glial fibrillary acidic protein-positive (GFAP+) astrocytes appear to be mainly localized in the explant [33]. Cultured explants were counterstained with DAPI, and the area occupied by the neuroblasts migrated out of the explants, here referred to as “migration area,” was quantified. A 25% reduction in the migration area was observed, when explants obtained from mice treated with anti Eps8 siRNA were compared with those obtained from mice treated with control siRNA (figs. 8D and E).

Discussion

ErbB4 is the only member of the ErbB family that exists in four alternative isoforms with the potential to mediate different biological functions. We previously chose a neuronal progenitor cell line (ST14A) as an *in vitro* model and demonstrated that the ability to induce cell migration is different in the four ErbB4 isoforms [21]. Here we used the same cellular system to identify - by microarray analysis - genes regulated during ErbB4 mediated migration.

We found a strong correlation between the high NRG1 induced migratory activity of JMb-cyt1 and JMa-cyt2 ErbB4 isoform expressing cells, and the expression of Eps8, which is an actin capping and bundling protein, initially identified as “EGFR-pathway substrate number 8” [22].

We hypothesized that Eps8 could play a role in mediating NRG1 induced migration. Indeed, this is the case: we found that transiently expressed ErbB4 and Eps8 synergized to mediate basal and NRG1 induced migration in ST14A cells. In addition, down-regulating Eps8 expression in ErbB4 expressing ST14A cells by siRNA treatment, significantly interfered with basal and ligand stimulated migration. In this respect, we did not observe differences when either both Eps8 isoforms, or only the 97 kDa form were switched off, suggesting that it is the full length Eps8 which significantly affects migration. We also saw a significant decrease in hepatocyte growth factor/scatter factor (HGF/SF) induced migration upon Eps8 interference, indicating that the role of Eps8 in the regulation of growth factor stimulated migration is not limited to NRG1.

HGF/SF triggers reorganization of the actin cytoskeleton in ST14A cells [34, 35]. Here we demonstrated, in the same cellular model, that organized stress fibers typically found in starved cells, are broken down and relocalized to lamellipodia upon NRG1 treatment. This difference is much less evident in Eps8 partially silenced cells. We could conclude that when Eps8 is down-regulated, there is less stress fiber formation upon starvation and less actin remodeling upon NRG1 stimulation. In line with these data, we previously demonstrated that in cerebellar granule neurons the lack of Eps8 renders the actin cytoskeleton less sensitive to

the remodeling action of ethanol [37].

Collectively, these findings indicate that Eps8 is an important relay downstream of receptor tyrosine kinases in regulating migration in neuronal progenitors.

The ability of Eps8 to regulate migration downstream of growth factor stimulation is not universal but is strictly cell type specific: migration is not impaired in fibroblasts derived from Eps8$^{-/-}$ mice (unpublished observation) and attempts in various cell lines to score an effect of Eps8 depletion on cellular migration failed [38, 39]. On the contrary, also migration of an oral squamous cell carcinoma [40-42] and of a lung carcinoma epithelial cell line [43] are sensitive to Eps8 expression levels. These findings are likely explained by the fact that Eps8 is a multimodular regulator of actin dynamics and its capability to influence the cell ability to migrate strongly depends on its spatio-temporal localization and interactions with specific proteins involved in the regulation of actin dynamics, an aspect that will be discussed later on.

In ST14A cells, stable expression of two particular ErbB4 isoforms up-regulates Eps8, which consequently participates in the migration induced by different growth factors. The correlation between specific ErbB4 isoform expression and Eps8 up-regulation is statistically significant. We can exclude clonal bias, since two representative stable clones for each ErbB4 isoform were chosen for the expression analysis and identical results were obtained.

Only two out of the four ErbB4 isoforms induce the Eps8 transcription: JMb-cyt1 and JMa-cyt2.

JMb-cyt1 isoform is a transmembrane receptor which contains, in the cytoplasmic region, a docking site for PI3K [14, 15] and E3 ubiquitin ligases [16-19]. We propose that its ability to activate PI3K signalling is involved in the augmentation of Eps8 protein since we observed that it is down-regulated after 96 hour of LY treatment. In agreement, JMb-cyt2 isoform does not increase Eps8 expression, because it does not activate directly PI3K pathway.

JMa-cyt2 isoform can be cleaved and releases a stable cytoplasmic fragment which can move into the nucleus and influences transcription [6-13]. We suggest that this pathway could

be involved in Eps8 transcription: obstructing γ-secretase activity, the level of Eps8 protein decreases after 72 hours of treatment. Accordingly, the JMa-cyt1 isoform does not increase Eps8 expression, because the intracellular fragment is degraded before entering into the nucleus [10, 17, 44].

One question that emerges is how Eps8 effect on migration might be regulated by growth factor stimulation. It has been shown that Eps8 function is regulated depending on the protein complex in which it enters: in a complex with Abi-1, Sos-1 and PI3K it activates Rac [23]; in a complex with Abi-1 alone, its actin barbed end activity is liberated [24]; instead, in a complex with Irsp53, Eps8 has a potent actin filament bundling activity [25]. Additionally, in neurons, Brain-Derived Neurotrophic Factor (BDNF) stimulation leads to Eps8 phosphorylation by MAPK which in turn regulates its interaction with Abi-1 and its association with F-actin [45]. Evidently, the spatio-temporal localization of Eps8 and its interaction with other proteins dictates its function and needs to be tightly controlled. Phosphorylation downstream of growth factor stimulation could be an efficient way to do so.

It has previously been shown that Eps8 is phosphorylated by growth factor stimulation and constitutively so in tumor cells [46]. We can speculate that the synergistic effect, which we observe upon overexpression of Eps8 and ErbB4 on cell migration, might be mediated by an increased capability to phosphorylate and thus regulate Eps8 function. This might not necessarily mean that Eps8 is a direct substrate of ErbB4 and indeed we didn’t observe a direct interaction between the two proteins (data not shown). One can also envision, that Eps8 might be phosphorylated by non-receptor tyrosine kinases like src [47], or serine/threonine kinases like MAPK [45] which can be activated upon ErbB4 stimulation. This would be in line with previous observations, that tyrosine phosphorylation of Eps8 upon EGF stimulation is a late event [22].

It has been already well demonstrated that endogenous ErbB4 has an important role in the migration of normal neuronal precursor cells from the medial ganglionic eminence to the

cortex [3] and from the SVZ to the OB [48]. On the contrary - to our knowledge - a role of Eps8 in the neuronal precursor cell migration has not been described to date, although its expression has been demonstrated in the central nervous system [49].

We show here that Eps8, like ErbB4, is expressed in the SVZ, in the RMS and in the OB and we verified the expression of the four ErbB4 isoforms in these regions (data not shown). To investigate the role of Eps8 in neuronal precursor cell migration, we down-regulated Eps8 by *in vivo* siRNA injection into the lateral ventricle, followed by *in vivo* electroporation. Through the analysis of primary cultures of *ex vivo* SVZ explants, we demonstrated that Eps8 down-regulation affects normal neuronal precursor migration.

In summary, our results demonstrate that Eps8 plays an important role in the migration of the neuronal progenitor cell line ST14A stably expressing ErbB4 and in the migratory activity of OB precursors endogenously expressing ErbB4 and Eps8. These findings underline the importance of proper actin remodeling in neuronal migration and its fine tuning by receptor tyrosine kinase mediated signaling cascades.

Further accurate studies and detailed morphological analyses of Eps8 expressing cells in the central nervous system will be necessary to better characterize its role *in vivo*.

Figure Legends

Figure 1 - Eps8 is highly expressed by stable clones expressing JMb-cyt1 or JMa-cyt2 ErbB4 isoform - *Panel A* - Stable clones, each expressing an ErbB4 isoform, and a pool of mock transfected cells (mock), were starved in 2% FBS DMEM and then stimulated or not with 5 nM NRG1. 12 hrs after stimulation, total RNA was isolated, reverse transcribed and subjected to qRT-PCR analysis. Results are presented as relative quantities, normalized against geometric means of two housekeeping genes amplified from the same cDNA, namely TBP and UbC. In the graphic, alternated black and white columns represent the mock sample and the stable clones expressing the different ErbB4 isoforms (summarized in Table B). Biological triplicate experiments were carried out in a technical triplicate. Values are expressed as mean + SEM. Statistical analysis demonstrates that B1 and A2 expressing clones have an Eps8 level which is significantly higher than mock cells (*$p \leq 0.05$, **$p \leq 0.01$, ***$p \leq 0.001$) and that NRG1 stimulation increases Eps8 transcript level only in the clone A2.1 ($p = 0.011$).

Table B - shows the list of the stable clones expressing the different ErbB4 isoforms and summarizes their migration activity following 18 hours 5nM NRG1 stimulation.

Figure 2 - Eps8 expression in ErbB4-ST14A stable cell clones - 30 µg total protein extract from stable cell clones, each expressing an ErbB4 isoform, were separated on a 10% acrylamide gel and blotted on a nitrocellulose membrane. The membrane was decorated with anti-ErbB4, anti-Eps8 and anti-β-actin antibodies. The two bands of 97 and 68 kDa represent the two Eps8 isoforms. A band of 180 kDa represents the full length ErbB4 receptor. The asterisks point to unspecific bands. Actin bands were used to assess comparable loading. The Eps8 expression level is comparable in the two independent clones expressing the same ErbB4 isoform and is not relative to the level of ErbB4 expression.

Figure 3 - Eps8 expression is down-regulated by PI3K inhibitor treatment in JMb-cyt1 expressing cells and by γ-secretase inhibitor treatment in JMa-cyt2 expressing cells.

The B1.15 stable clone (expressing the JMb-cyt1 ErbB4 isoform, upper panel) and the A2.1 stable clone (expressing the JMa-cyt2 ErbB4 isoform, lower panel), were treated with DMSO (the solvent) or 10 µM DAPT (γ-secretase inhibitor) or 10 µM LY294002 (PI3K inhibitor); total proteins were extracted at different time intervals, between 24 and 96 hours after treatment. Equal amounts of total protein extracts were separated on 10% acrylamide gels and blotted on nitrocellulose membranes. The membranes were decorated with anti-Eps8 antibody and with anti-ErbB2, anti-ErbB3 and anti-actin antibodies, to exclude non-specific effects on protein expression.

The Eps8 level decreases in B1.15 cells 96 hours after PI3K inhibitor treatment, in A2.1 cells 72 hours after γ-secretase inhibitor treatment.

Figure 4 - JMa-cyt2 ErbB4 expressing cells, stimulated with NRG1, up-regulate Eps8 protein - In time course assays, the B1.15 stable clone, expressing JMb-cyt1 ErbB4 isoform (*Panel A*), and the A2.1 stable clone, expressing JMa-cyt2 ErbB4 isoform (*Panels B and C*), previously starved for 24 hours in serum free medium, were stimulated with 5 nM NRG1 for different time points. In Panel A and B the time course stimulation ranged between 15 and 120 minutes, in Panel C between 30 minutes and 18 hours. Total protein extracts were separated on 8 % acrylamide gels and blotted on nitrocellulose membranes. The membranes were decorated with anti-Eps8, anti P-ErbB4 (tyr 1284) and anti-ErbB4 antibodies. B1.15 cells display a high level of Eps8 protein, which doesn't increase after ligand stimulation, whereas A2.1 cells express a lower level of Eps8 protein which increases 45 minutes later.

Figure 5 - ErbB4 and Eps8 transient expression confers to the cells the ability to migrate - ST14A mock cells were transiently co-transfected with the following combination of plasmids: pCEV + pIRESpuro2 (mock); pCEV + pIRESpuro2-ErbB4-JMb-cyt1 (ErbB4); pCEV-Eps8 + pIRESpuro2-ErbB4-JMb-cyt1 (ErbB4-Eps8); pCEV-Eps8 + pIRESpuro2 (Eps8). Forty-eight hours after transfection, Transwell assays were performed in 2% FBS DMEM either without (white bars) or with (black bars) 5 nM NRG1. Migration was calculated as percentage of total migrated cells as described in Materials and Methods. Biological triplicate experiments were carried out in a technical triplicate. Data are represented as means + SEM. Statistical analysis shows that ErbB4 alone increases migration activity, but in combination with Eps8, the effect is significantly higher (**$p \leq 0.01$, ***$p \leq 0.001$); moreover, it shows a statistically significant increase of basal migration when comparing mock cells with cells co-expressing ErbB4 and Eps8 ($p = 0.004$).

Figure 6 - Eps8 down-regulation interferes with NRG1-induced migration - *Panel A* - Set up of siRNA transfection conditions: A2.1 cells were transfected with 20 nM control scramble siRNA or anti-Eps8 specific siRNAs #86, #85 or #84. Total proteins were extracted 48 hrs after transfection and analyzed by western blot. The membrane was decorated with anti-Eps8 and anti-β-actin antibodies to assess comparable loading. The two bands of 97 and 68 kDa represent the two isoforms of Eps8. The asterisk points to an unspecific band useful to confirm the equity in loading amount. *Panel B* - A2.1 cells were transfected with 10 nM control scramble siRNA, #85/86 pool anti-Eps8 siRNA, or #84 siRNA alone. The #85 and #86 siRNA pool down-regulates both Eps8 isoforms, the #84 siRNA only the 97kDa one. Total proteins were analyzed as described in Panel A. *Panel C* - A2.1 and B1.15 cells were transfected with 10 nM control scramble siRNA or #85/86 pool anti-Eps8 siRNA; total RNA was extracted 48 hrs later and subjected to qRT-PCR analysis for Eps8 expression. The quantity of Eps8 transcript in rat stomach was chosen as a calibrator. Data (represented as means + SEM)

show a reduction of Eps8 after siRNA treatment (*p < 0.01). *Panels D - E* - Two clones representative of two ErbB4 isoforms (JMb-cyt1, clone B1.15, panel D and JMa-cyt2, clone A2.1, panel E) were transiently transfected with scramble 10 nM siRNA (CTR), or a pool of anti-Eps8 siRNAs (#85 and #86), or #84 alone. 48 hrs later, transfected cells were assayed for migration: Transwell assays were performed in 2% FBS DMEM either without (white bars) or with (black bars) 5 nM NRG1. In the graphic, for each experimental point, the migrated cells are expressed as percentage of the total number of migrated cells. Biological triplicate experiments were carried out in technical triplicate. Data represent means + SEM (*p≤0.05, ***p≤0.001).

Figure 7 - NRG1 induces reorganization of actin cytoskeleton, which is reduced by Eps8 silencing - A2.1 cells were transiently transfected with actin M-cherry alone or co-transfected with actin M-cherry and 10nM scramble siRNA (CTR), or #85/86 pool of anti-Eps8 siRNAs (Eps8). Serum starved cells were stimulated (+) or not (-) with NRG1, and analyzed for actin cytoskeleton organization. Three independent experiments were performed; for each sample, at least 100 cells were scored and the percentage of cells displaying stress fiber actin organization was calculated. *Panel A* - Graphic shows the media of three independent experiments + SEM (*p≤0.05, **p≤0.01). Black bars=percentage of cells with actin organized in stress fibers, white bars= percentage of cells with disorganized actin.

Panel B – Representative images of cells in the different treatment conditions described in panel A. Scale bar = 20 µm.

Figure 8 - Eps8 is expressed in the SVZ and along the RMS and its down-regulation inhibits migration of olfactory bulb neuronal precursors

Panel A - Schematic representation of a sagittal forebrain slice of postnatal day 5 (P5) mice. (a) SVZ: the SVZ of the lateral ventricle; (b) p-RMS: the posterior part of the RMS; (c) a-RMS:

the anterior part of the RMS; (d) OB: the OB layers surrounding the a-RMS. *Panel B* - Western blot analysis of total proteins extracted from mouse tissue microdissections obtained from P5 SVZ, p-RMS, a-RMS, OB and from adult OB. The membrane was decorated with anti-ErbB4, anti-Eps8 and anti-β-actin antibodies. A band of 180 kDa represents the full length ErbB4 receptor; the two bands of 97 and 68 KDa represent the two Eps8 isoforms. The asterisks point to unspecific bands. Actin bands were used to assess comparable loading.

Panel C - Total protein extracts from 4 representative explants obtained from animals electroporated *in vivo* with scramble siRNA ("siRNA CTR") or siRNA directed versus Eps8 ("siRNA Eps8", see material and methods for details) have been separated on a 10% acrylamide gel and blotted on a nitrocellulose membrane. To assess Eps8 down-regulation, the membrane was decorated with anti-Eps8 primary antibody. β-actin bands were used to assess comparable loading. *Panel D* - Digitalized images representative of the migration area of SVZ explants stained with DAPI, obtained from mice electroporated with scramble siRNA (siRNA CTR) or siRNA directed versus Eps8 (siRNA Eps8). Scale bar: 100µm. *Panel E* - Quantification of the migration area calculated on digitalized images as the surface covered by DAPI nuclear staining, excluding the tissue explant area by means of Image J software. The procedure has been carried out in a blind manner. The experiment was repeated three times, using 4-5 mice for each treatment (explant number= 119 out of 15 animals for CTR siRNA; n=104 out of 14 animals for Eps8 siRNA). Data are represented as means + SEM. T-test was used to compare differences between treatments. ** $p < 0,01$ ($p=0.0019$).

SUPPLEMENTARY FIGURES

Table S1 - List of modulated genes obtained by the comparison between NRG1 stimulated A2.12 ST14A cells versus NRG1 stimulated mock cells. **–** Cells were treated with 5 nM NRG1 for 12 hrs prior to harvesting of RNA for analysis on Agilent Whole Rat Genome microarrays. Rosetta Resolver error model was applied to A2.12 ST14A cells versus mock. Values are based on duplicate arrays with dye-swap, selected genes have a Fold Change greater than 2.

Figure S1 - Functional clustering annotation of regulated genes. The list of ErbB4-regulated genes, obtained from microarray analysis, was analyzed using the functional annotation clustering tool in DAVID. This tool calculates enrichment score based on the overall EASE scores of all enriched annotation terms. Three representative clusters are shown here; the corresponding heatmaps are shown in figure S2.

Figure S2 - Representative heatmaps of cellular motility related genes in ErbB4-overexpressing cells. These heatmaps correspond to the functionally annotated gene clusters, shown in figure S1. Green color indicates the relationship of a gene with a particular Gene Ontology (GO) term.

Figure S3 - Protein network in ErbB4-expressing cells. The list of gene products (Table S1), obtained from gene expression profiling experiments, showing 2 fold or greater overexpression in ErbB4 expressing cells, was analyzed using Metacore software. Here is shown one representative network containing ErbB4 and some regulated genes involved in cell migration. As indicated in the legend, red spots correspond to up-regulated, blue spots to down-regulated genes.

Table S2 - List of candidate genes analyzed by quantitative RT-PCR (qRT-PCR) - Gene expression regulation of all genes, except Msln and Tmsbl1, was validated by qRT-PCR.

Acknowledgements. The plasmid to express actin M-cherry was kindly provided by prof. Kenneth Yamada (NIH/NIDCR). We are grateful to Enrico Martina, Francesco Rua, Giulia Garaffo, and Sara Gnavi for their contribute during their master degree thesis. This work was supported by grants from the Ministero Italiano dell'Università e della Ricerca (PRIN 2007) Regione Piemonte ("Bando Ricerca Sanitaria Finalizzata"), Università di Torino. N.O. is recipient of grants from Associazione Italiana per la Ricerca sul Cancro (AIRC), Cariplo and Compagnia di San Paolo di Torino. F.F. and G.C. are supported by grants of Compagnia di San Paolo di Torino.

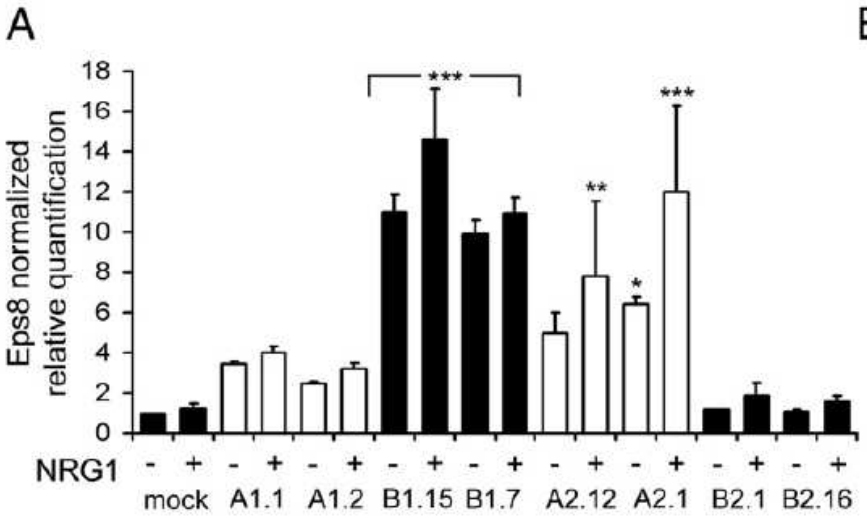

B

ISOFORM	STABLE CLONES	NRG1 induced migration
JMa-cyt1 (A1)	A1.1	+
	A1.2	
JMb-cyt1 (B1)	B1.7	+++
	B1.15	
JMa-cyt2 (A2)	A2.1	++
	A2.12	
JMb-cyt2 (B2)	B2.1	+
	B2.16	
empty vector	mock	–

Figure 1

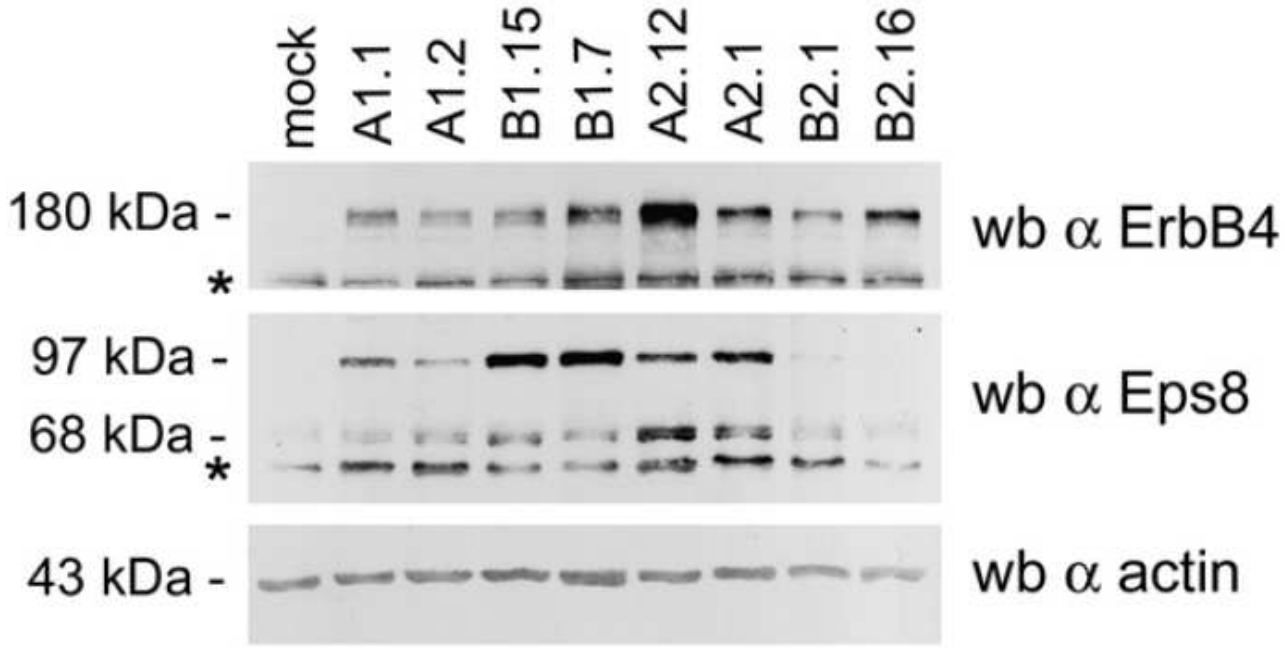
mock
A1.1
A1.2
B1.15
B1.7
A2.12
A2.1
B2.1
B2.16
180 kDa -
*
wb α ErbB4
97 kDa -
68 kDa -
*
wb α Eps8
43 kDa -
wb α actin

Figure 2

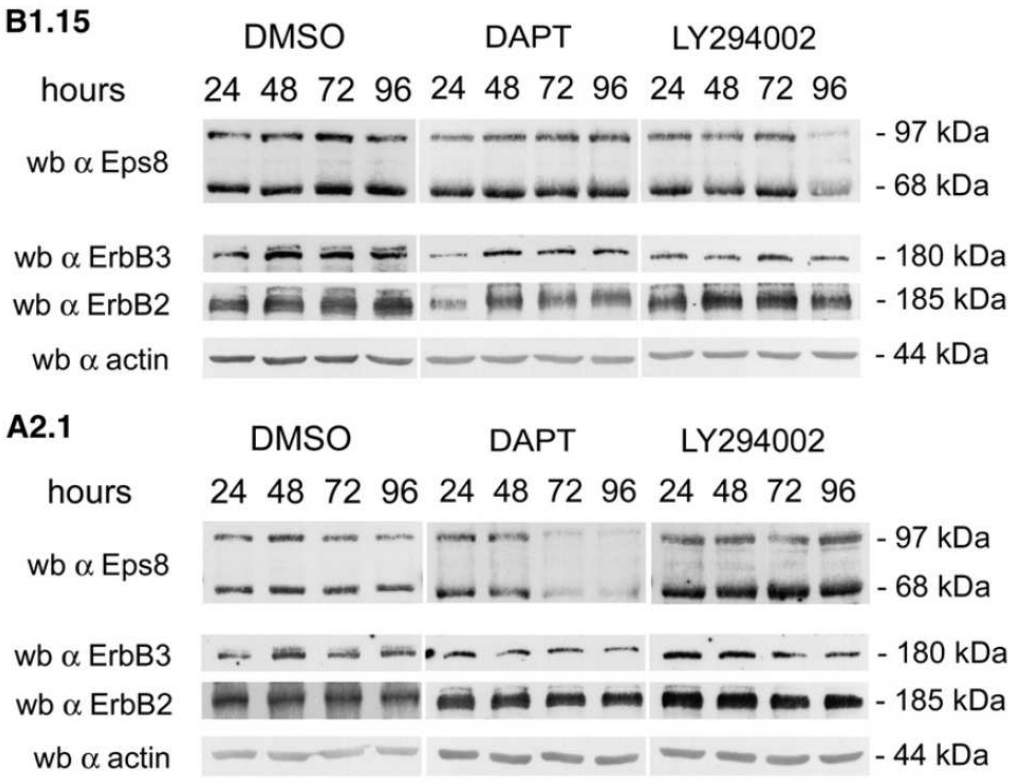
B1.15
DMSO
DAPT
LY294002
hours
24 48 72 96 24 48 72 96 24 48 72 96
wb α Eps8
- 97 kDa
- 68 kDa
wb α ErbB3
- 180 kDa
wb α ErbB2
- 185 kDa
wb α actin
- 44 kDa
A2.1
DMSO
DAPT
LY294002
hours
24 48 72 96 24 48 72 96 24 48 72 96
wb α Eps8
- 97 kDa
- 68 kDa
wb α ErbB3
- 180 kDa
wb α ErbB2
- 185 kDa
wb α actin
- 44 kDa

Figure 3

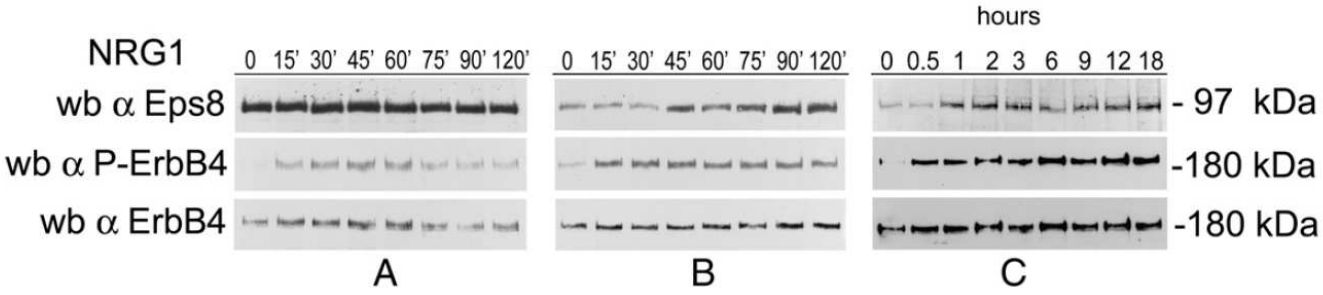
hours
NRG1
0 15' 30' 45' 60' 75' 90' 120'
0 15' 30' 45' 60' 75' 90' 120'
0 0.5 1 2 3 6 9 12 18
wb α Eps8
wb α P-ErbB4
wb α ErbB4
- 97 kDa
-180 kDa
-180 kDa
A
B
C

Figure 4

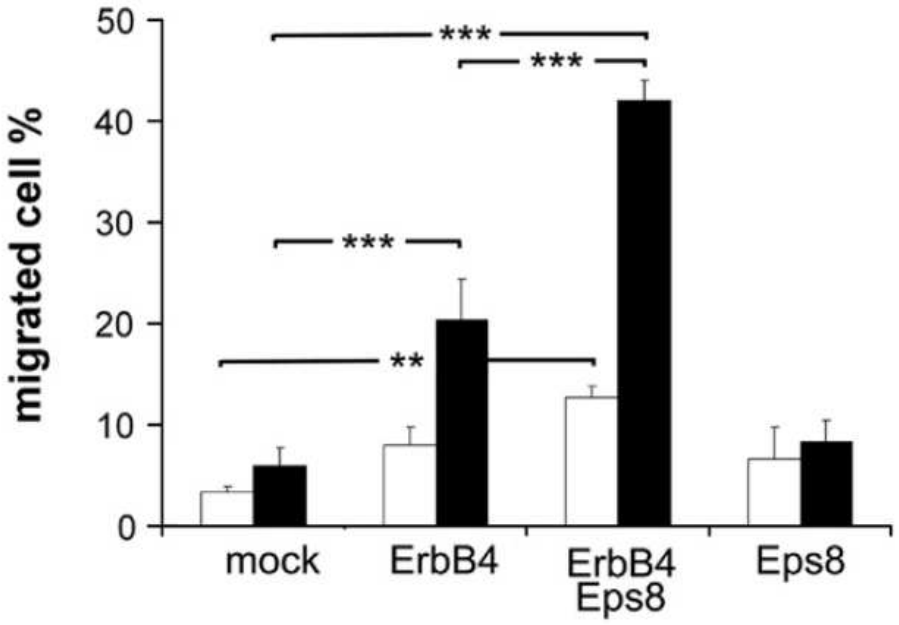

Figure 5

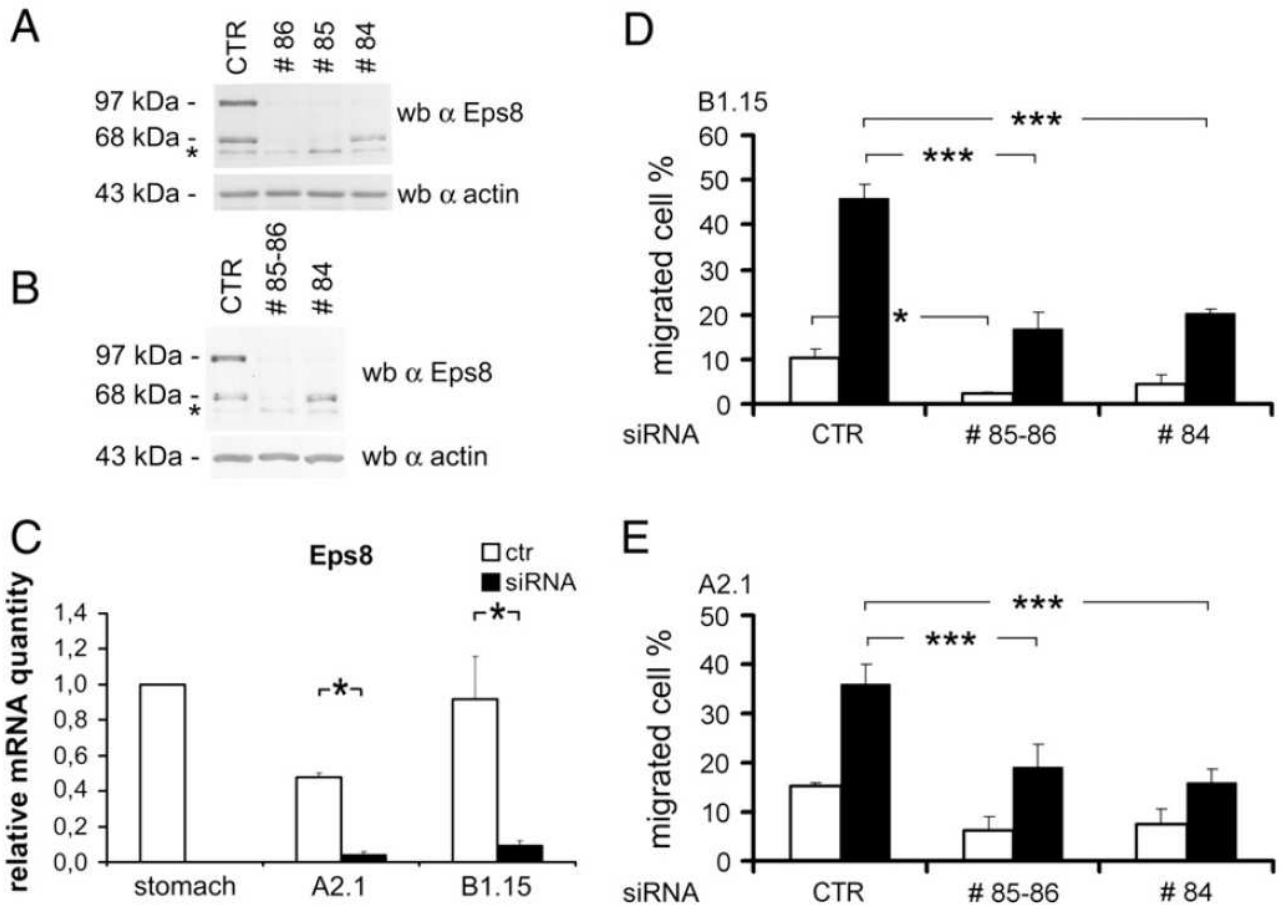
A
CTR
86
85
84
97 kDa -
68 kDa -
*
wb α Eps8
43 kDa -
wb α actin
B
CTR
85-86
84
97 kDa -
68 kDa -
*
wb α Eps8
43 kDa -
wb α actin
C
Eps8
ctr
siRNA
relative mRNA quantity
1,4
1,2
1,0
0,8
0,6
0,4
0,2
0,0
*
*
stomach
A2.1
B1.15
D
B1.15
migrated cell %
60
50
40
30
20
10
0
***
***
*
siRNA
CTR
85-86
84
E
A2.1
migrated cell %
50
40
30
20
10
0
***
***
siRNA
CTR
85-86
84

Figure 6

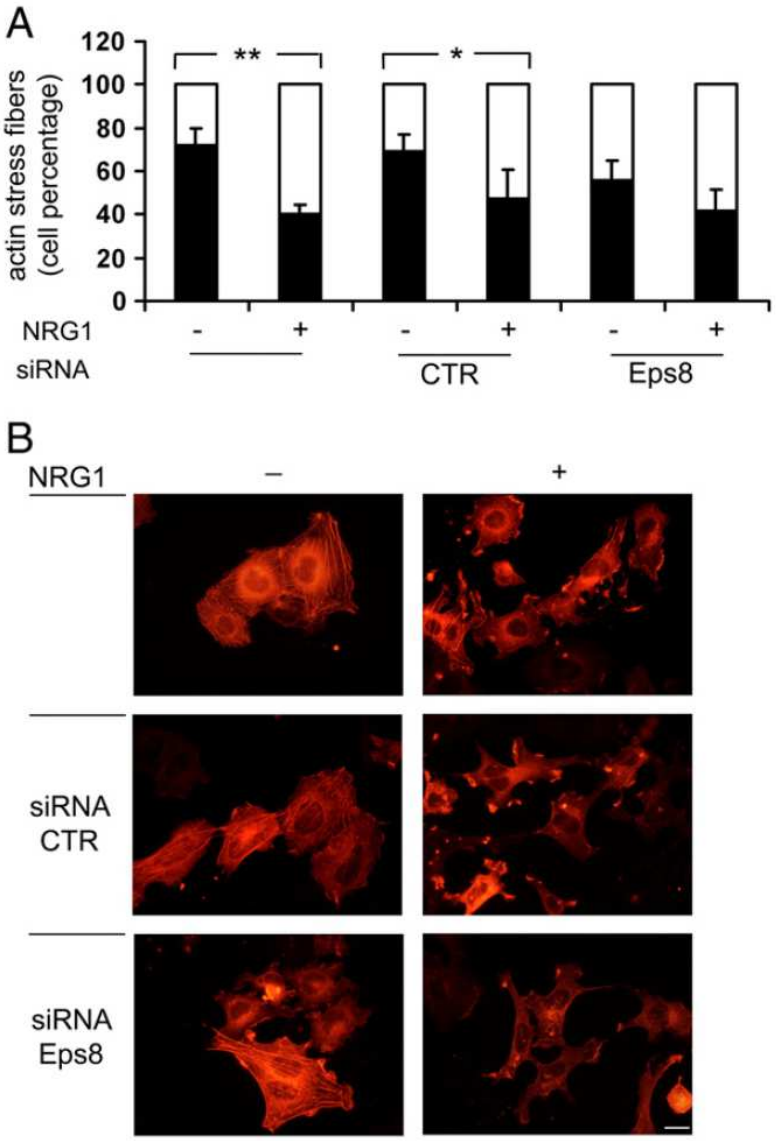
A
actin stress fibers
(cell percentage)
120
100
80
60
40
20
0
**
*
NRG1
-
+
-
+
-
+
siRNA
CTR
Eps8
B
NRG1
–
+
siRNA
CTR
siRNA
Eps8

Figure 7

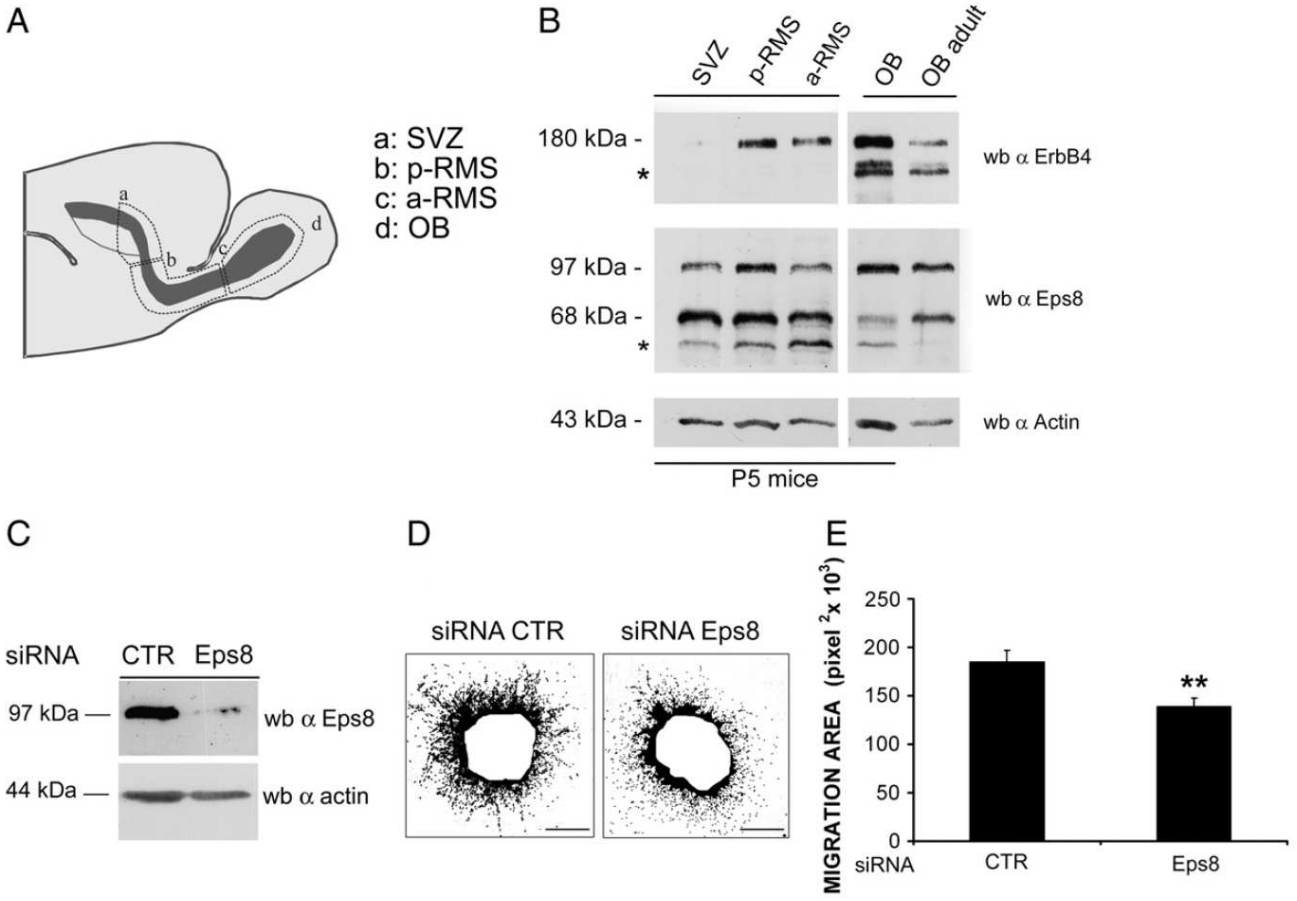
A
a: SVZ
b: p-RMS
c: a-RMS
d: OB
B
SVZ
p-RMS
a-RMS
OB
OB adult
180 kDa -
*
wb α ErbB4
97 kDa -
68 kDa -
*
wb α Eps8
43 kDa -
wb α Actin
P5 mice
C
siRNA
CTR
Eps8
97 kDa
wb α Eps8
44 kDa
wb α actin
D
siRNA CTR
siRNA Eps8
E
MIGRATION AREA (pixel 2x 10^3)
250
200
150
100
50
0
**
siRNA
CTR
Eps8

Figure 8

Annotation Cluster 15	Enrichment Score: 2.03			Count	P_Value	Fold Change	Benjamini
SP_PIR_KEYWORDS	cell adhesion	RT		14	1.5E-3	2.8E0	1.1E-1
GOTERM_BP_FAT	cell adhesion	RT		18	2.3E-2	1.8E0	3.5E-1
GOTERM_BP_FAT	biological adhesion	RT		18	2.3E-2	1.8E0	3.5E-1

Annotation Cluster 20	Enrichment Score: 1.78			Count	P_Value	Fold Change	Benjamini
GOTERM_BP_FAT	locomotory behavior	RT		13	1.9E-3	2.9E0	9.7E-2
GOTERM_BP_FAT	adult locomotory behavior	RT		5	4.5E-2	3.7E0	4.7E-1
GOTERM_BP_FAT	adult behavior	RT		6	5.5E-2	2.9E0	5.1E-1

Annotation Cluster 61	Enrichment Score: 0.81			Count	P_Value	Fold Change	Benjamini
GOTERM_BP_FAT	cytoskeleton organization	RT		12	8.4E-2	1.7E0	6.1E-1
GOTERM_BP_FAT	microtubule cytoskeleton organization	RT		5	1.8E-1	2.3E0	7.9E-1
GOTERM_BP_FAT	microtubule-based process	RT		7	2.5E-1	1.7E0	8.6E-1

Figure S1

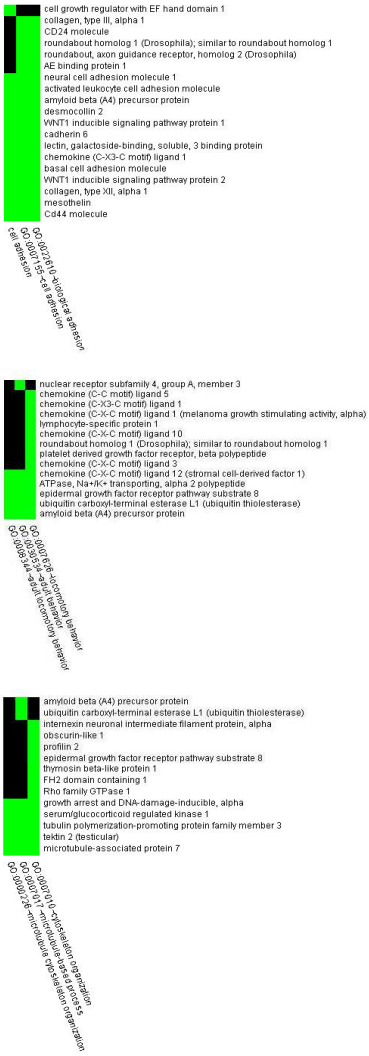
cell growth regulator with EF hand domain 1
collagen, type III, alpha 1
CD24 molecule
roundabout homolog 1 (Drosophila); similar to roundabout homolog 1
roundabout, axon guidance receptor, homolog 2 (Drosophila)
AE binding protein 1
neural cell adhesion molecule 1
activated leukocyte cell adhesion molecule
amyloid beta (A4) precursor protein
desmocollin 2
WNT1 inducible signaling pathway protein 1
cadherin 6
lectin, galactoside-binding, soluble, 3 binding protein
chemokine (C-X3-C motif) ligand 1
basal cell adhesion molecule
WNT1 inducible signaling pathway protein 2
collagen, type XII, alpha 1
mesothelin
Cd44 molecule
GO:0007155~cell adhesion
GO:0022610~biological adhesion
cell adhesion
nuclear receptor subfamily 4, group A, member 3
chemokine (C-C motif) ligand 5
chemokine (C-X3-C motif) ligand 1
chemokine (C-X-C motif) ligand 1 (melanoma growth stimulating activity, alpha)
lymphocyte-specific protein 1
chemokine (C-X-C motif) ligand 10
roundabout homolog 1 (Drosophila); similar to roundabout homolog 1
platelet derived growth factor receptor, beta polypeptide
chemokine (C-X-C motif) ligand 3
chemokine (C-X-C motif) ligand 12 (stromal cell-derived factor 1)
ATPase, Na+/K+ transporting, alpha 2 polypeptide
epidermal growth factor receptor pathway substrate 8
ubiquitin carboxyl-terminal esterase L1 (ubiquitin thiolesterase)
amyloid beta (A4) precursor protein
GO:0007610~behavior
GO:0008150~biological_process
GO:0050890~cognition
amyloid beta (A4) precursor protein
ubiquitin carboxyl-terminal esterase L1 (ubiquitin thiolesterase)
internexin neuronal intermediate filament protein, alpha
obscurin-like 1
profilin 2
epidermal growth factor receptor pathway substrate 8
thymosin beta-like protein 1
FH2 domain containing 1
Rho family GTPase 1
growth arrest and DNA-damage-inducible, alpha
serum/glucocorticoid regulated kinase 1
tubulin polymerization-promoting protein family member 3
tektin 2 (testicular)
microtubule-associated protein 7
GO:0007010~cytoskeleton organization
GO:0007017~microtubule-based process
GO:0000226~microtubule cytoskeleton organization

Figure S2

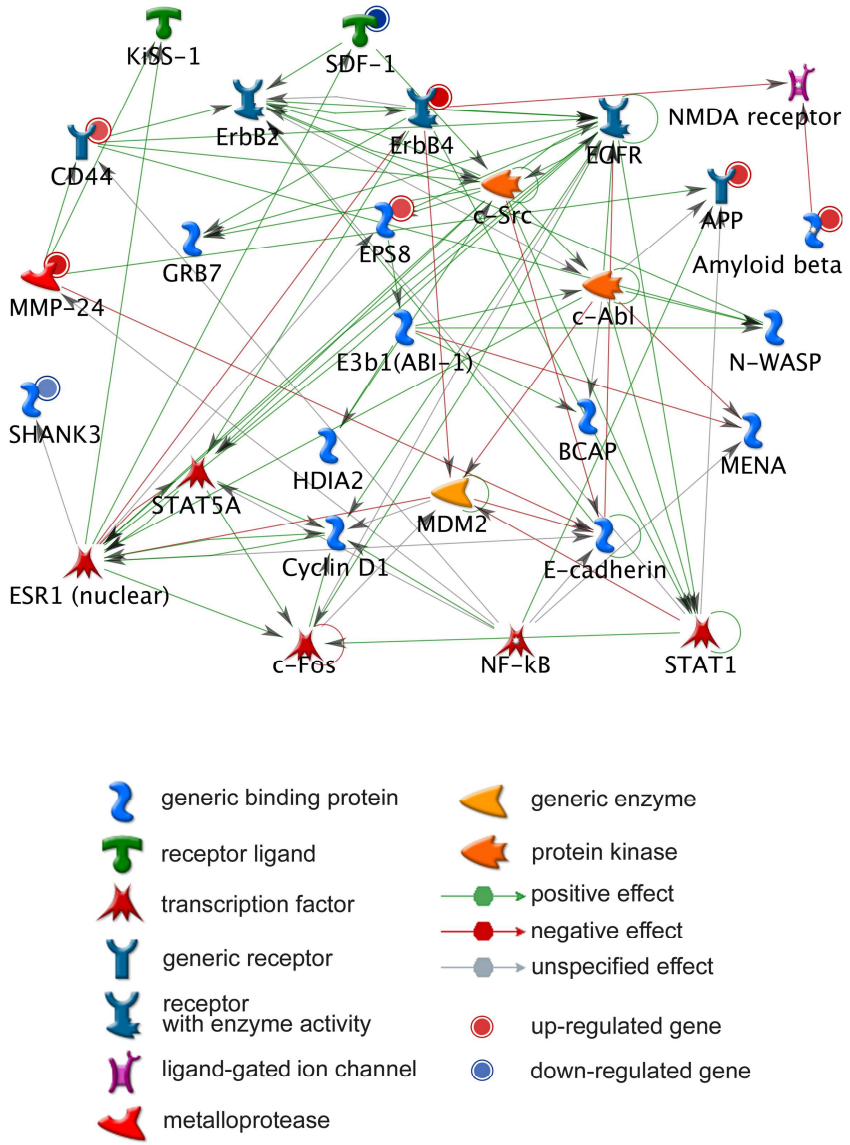
KiSS-1
SDF-1
ErbB2
ErbB4
EGFR
NMDA receptor
CD44
c-Src
APP
Amyloid beta
GRB7
EPS8
MMP-24
c-Abl
E3b1(ABl-1)
N-WASP
SHANK3
BCAP
MENA
HDIA2
STAT5A
MDM2
Cyclin D1
E-cadherin
ESR1 (nuclear)
c-Fos
NF-kB
STAT1
generic binding protein
receptor ligand
transcription factor
generic receptor
receptor with enzyme activity
ligand-gated ion channel
metalloprotease
generic enzyme
protein kinase
positive effect
negative effect
unspecified effect
up-regulated gene
down-regulated gene

Figure S3

number	gene	abbreviation
1	Thymosin beta-like protein 1	*Tmsbl1*
2	Stathmin-like 4	*Stmn4*
3	Mesothelin	*Msln*
4	Matrix metallopeptidase 24	*Mmp24*
5	Fibroblast growth factor 5	*Fgf5*
6	Epidermal growth factor receptor pathway substrate 8	*Eps8*
7	Similar to Kelch-like 13	*Klhl13*
8	Chemokine (C-X-C motif) ligand 12/ stromal cell-derived factor 1	*Cxcl12/SDF-1*

Table S2

References

[1] H.T. Ghashghaei, C. Lai, E.S. Anton, Neuronal migration in the adult brain: are we there yet?, Nat Rev Neurosci 8 (2007) 141-151.

[2] L. Mei, W.C. Xiong, Neuregulin 1 in neural development, synaptic plasticity and schizophrenia, Nat Rev Neurosci 9 (2008) 437-452.

[3] N. Flames, J.E. Long, A.N. Garratt, T.M. Fischer, M. Gassmann, C. Birchmeier, C. Lai, J.L. Rubenstein, O. Marin, Short- and long-range attraction of cortical GABAergic interneurons by neuregulin-1, Neuron 44 (2004) 251-261.

[4] B. Linggi, G. Carpenter, ErbB receptors: new insights on mechanisms and biology, Trends Cell Biol 16 (2006) 649-656.

[5] Q.C. Cheng, O. Tikhomirov, W. Zhou, G. Carpenter, Ectodomain cleavage of ErbB-4: characterization of the cleavage site and m80 fragment, J Biol Chem 278 (2003) 38421-38427.

[6] C.Y. Ni, M.P. Murphy, T.E. Golde, G. Carpenter, gamma -Secretase cleavage and nuclear localization of ErbB-4 receptor tyrosine kinase, Science 294 (2001) 2179-2181.

[7] H.J. Lee, K.M. Jung, Y.Z. Huang, L.B. Bennett, J.S. Lee, L. Mei, T.W. Kim, Presenilin-dependent gamma-secretase-like intramembrane cleavage of ErbB4, J Biol Chem 277 (2002) 6318-6323.

[8] A. Komuro, M. Nagai, N.E. Navin, M. Sudol, WW domain-containing protein YAP associates with ErbB-4 and acts as a co-transcriptional activator for the carboxyl-terminal fragment of ErbB-4 that translocates to the nucleus, J Biol Chem 278 (2003) 33334-33341.

[9] C.C. Williams, J.G. Allison, G.A. Vidal, M.E. Burow, B.S. Beckman, L. Marrero, F.E. Jones, The ERBB4/HER4 receptor tyrosine kinase regulates gene expression by functioning as a STAT5A nuclear chaperone, J Cell Biol 167 (2004) 469-478.

[10] J.A. Maatta, M. Sundvall, T.T. Junttila, L. Peri, V.J. Laine, J. Isola, M. Egeblad, K. Elenius, Proteolytic cleavage and phosphorylation of a tumor-associated ErbB4 isoform promote ligand-independent survival and cancer cell growth, Mol Biol Cell 17 (2006) 67-79.

[11] S.P. Sardi, J. Murtie, S. Koirala, B.A. Patten, G. Corfas, Presenilin-dependent ErbB4 nuclear signaling regulates the timing of astrogenesis in the developing brain, Cell 127 (2006) 185-197.

[12] F.E. Jones, HER4 intracellular domain (4ICD) activity in the developing mammary gland and breast cancer, J Mammary Gland Biol Neoplasia 13 (2008) 247-258.

[13] M. Sundvall, V. Veikkolainen, K. Kurppa, Z. Salah, D. Tvorogov, E.J. van Zoelen, R. Aqeilan, K. Elenius, Cell Death or Survival Promoted by Alternative Isoforms of ErbB4, Mol Biol Cell.

[14] K. Elenius, C.J. Choi, S. Paul, E. Santiestevan, E. Nishi, M. Klagsbrun, Characterization of a naturally occurring ErbB4 isoform that does not bind or activate phosphatidyl inositol 3-kinase, Oncogene 18 (1999) 2607-2615.

[15] V. Kainulainen, M. Sundvall, J.A. Maatta, E. Santiestevan, M. Klagsbrun, K. Elenius, A natural ErbB4 isoform that does not activate phosphoinositide 3-kinase mediates proliferation but not survival or chemotaxis, J Biol Chem 275 (2000) 8641-8649.

[16] J. Omerovic, L. Santangelo, E.M. Puggioni, J. Marrocco, C. Dall'Armi, C. Palumbo, F. Belleudi, L. Di Marcotullio, L. Frati, M.R. Torrisi, G. Cesareni, A. Gulino, M. Alimandi, The E3 ligase Aip4/Itch ubiquitinates and targets ErbB-4 for degradation, FASEB J 21 (2007) 2849-2862.

[17] M. Sundvall, A. Korhonen, I. Paatero, E. Gaudio, G. Melino, C.M. Croce, R.I. Aqeilan, K. Elenius, Isoform-specific monoubiquitination, endocytosis, and degradation of alternatively spliced ErbB4 isoforms, Proc Natl Acad Sci U S A 105 (2008) 4162-4167.

[18] Feng, The E3 Ubiquitin Ligase WWP1 Selectively Targets HER4 and Its

Proteolytically Derived Signaling Isoforms for Degradation , MOLECULAR AND CELLULAR BIOLOGY 29 (2009) 892–906.

[19] F. Zeng, J. Xu, R.C. Harris, Nedd4 mediates ErbB4 JM-a/CYT-1 ICD ubiquitination and degradation in MDCK II cells, FASEB J 23 (2009) 1935-1945.

[20] E. Cattaneo, L. Conti, Generation and characterization of embryonic striatal conditionally immortalized ST14A cells, J Neurosci Res 53 (1998) 223-234.

[21] G. Gambarotta, D. Garzotto, E. Destro, B. Mautino, C. Giampietro, S. Cutrupi, C. Dati, E. Cattaneo, A. Fasolo, I. Perroteau, ErbB4 expression in neural progenitor cells (ST14A) is necessary to mediate neuregulin-1beta1-induced migration, J Biol Chem 279 (2004) 48808-48816.

[22] F. Fazioli, L. Minichiello, V. Matoska, P. Castagnino, T. Miki, W.T. Wong, P.P. Di Fiore, Eps8, a substrate for the epidermal growth factor receptor kinase, enhances EGF-dependent mitogenic signals, EMBO J 12 (1993) 3799-3808.

[23] G. Scita, J. Nordstrom, R. Carbone, P. Tenca, G. Giardina, S. Gutkind, M. Bjarnegard, C. Betsholtz, P.P. Di Fiore, EPS8 and E3B1 transduce signals from Ras to Rac, Nature 401 (1999) 290-293.

[24] A. Disanza, M.F. Carlier, T.E. Stradal, D. Didry, E. Frittoli, S. Confalonieri, A. Croce, J. Wehland, P.P. Di Fiore, G. Scita, Eps8 controls actin-based motility by capping the barbed ends of actin filaments, Nat Cell Biol 6 (2004) 1180-1188.

[25] A. Disanza, S. Mantoani, M. Hertzog, S. Gerboth, E. Frittoli, A. Steffen, K. Berhoerster, H.J. Kreienkamp, F. Milanesi, P.P. Di Fiore, A. Ciliberto, T.E. Stradal, G. Scita, Regulation of cell shape by Cdc42 is mediated by the synergic actin-bundling activity of the Eps8-IRSp53 complex, Nat Cell Biol 8 (2006) 1337-1347.

[26] B. Mautino, L. Dalla Costa, G. Gambarotta, I. Perroteau, A. Fasolo, C. Dati, Bioactive recombinant neuregulin-1, -2, and -3 expressed in Escherichia coli, Protein Expr Purif 35 (2004) 25-31.

[27] S. Zhao, R.D. Fernald, Comprehensive algorithm for quantitative real-time polymerase chain reaction, J Comput Biol 12 (2005) 1047-1064.

[28] J. Vandesompele, K. De Preter, F. Pattyn, B. Poppe, N. Van Roy, A. De Paepe, F. Speleman, Accurate normalization of real-time quantitative RT-PCR data by geometric averaging of multiple internal control genes, Genome Biol 3 (2002) RESEARCH0034.

[29] J. Hellemans, G. Mortier, A. De Paepe, F. Speleman, J. Vandesompele, qBase relative quantification framework and software for management and automated analysis of real-time quantitative PCR data, Genome Biol 8 (2007) R19.

[30] M.W. Pfaffl, A. Tichopad, C. Prgomet, T.P. Neuvians, Determination of stable housekeeping genes, differentially regulated target genes and sample integrity: BestKeeper--Excel-based tool using pair-wise correlations, Biotechnol Lett 26 (2004) 509-515.

[31] T. Miki, T.P. Fleming, M. Crescenzi, C.J. Molloy, S.B. Blam, S.H. Reynolds, S.A. Aaronson, Development of a highly efficient expression cDNA cloning system: application to oncogene isolation, Proc Natl Acad Sci U S A 88 (1991) 5167-5171.

[32] C. Boutin, S. Diestel, A. Desoeuvre, M.C. Tiveron, H. Cremer, Efficient in vivo electroporation of the postnatal rodent forebrain, PLoS One 3 (2008) e1883.

[33] D. Garzotto, P. Giacobini, T. Crepaldi, A. Fasolo, S. De Marchis, Hepatocyte growth factor regulates migration of olfactory interneuron precursors in the rostral migratory stream through Met-Grb2 coupling, J Neurosci 28 (2008) 5901-5909.

[34] E. Cacci, M. Salani, S. Anastasi, I. Perroteau, G. Poiana, S. Biagioni, G. Augusti-Tocco, Hepatocyte growth factor stimulates cell motility in cultures of the striatal progenitor cells ST14A, J Neurosci Res 74 (2003) 760-768.

[35] C. Soldati, S. Biagioni, G. Poiana, G. Augusti-Tocco, beta-Catenin and actin reorganization in HGF/SF response of ST14A cells, J Neurosci Res 86 (2008) 1044-1052.

[36] H.T. Ghashghaei, J. Weber, L. Pevny, R. Schmid, M.H. Schwab, K.C. Lloyd, D.D. Eisenstat, C. Lai, E.S. Anton, The role of neuregulin-ErbB4 interactions on the proliferation and organization of cells in the subventricular zone, Proc Natl Acad Sci U S A 103 (2006) 1930-1935.

[37] N. Offenhauser, D. Castelletti, L. Mapelli, B.E. Soppo, M.C. Regondi, P. Rossi, E. D'Angelo, C. Frassoni, A. Amadeo, A. Tocchetti, B. Pozzi, A. Disanza, D. Guarnieri, C. Betsholtz, G. Scita, U. Heberlein, P.P. Di Fiore, Increased ethanol resistance and consumption in Eps8 knockout mice correlates with altered actin dynamics, Cell 127 (2006) 213-226.

[38] R.M. Katso, O.E. Pardo, A. Palamidessi, C.M. Franz, M. Marinov, A. De Laurentiis, J. Downward, G. Scita, A.J. Ridley, M.D. Waterfield, A. Arcaro, Phosphoinositide 3-Kinase C2beta regulates cytoskeletal organization and cell migration via Rac-dependent mechanisms, Mol Biol Cell 17 (2006) 3729-3744.

[39] T. Welsch, K. Endlich, T. Giese, M.W. Buchler, J. Schmidt, Eps8 is increased in pancreatic cancer and required for dynamic actin-based cell protrusions and intercellular cytoskeletal organization, Cancer Lett 255 (2007) 205-218.

[40] H. Wang, V. Patel, H. Miyazaki, J.S. Gutkind, W.A. Yeudall, Role for EPS8 in squamous carcinogenesis, Carcinogenesis 30 (2009) 165-174.

[41] H. Wang, M.T. Teh, Y. Ji, V. Patel, S. Firouzabadian, A.A. Patel, J.S. Gutkind, W.A. Yeudall, EPS8 upregulates FOXM1 expression, enhancing cell growth and motility, Carcinogenesis 31 1132-1141.

[42] L.F. Yap, V. Jenei, C.M. Robinson, K. Moutasim, T.M. Benn, S.P. Threadgold, V. Lopes, W. Wei, G.J. Thomas, I.C. Paterson, Upregulation of Eps8 in oral squamous cell carcinoma promotes cell migration and invasion through integrin-dependent Rac1 activation, Oncogene 28 (2009) 2524-2534.

[43] T.P. Yang, H.L. Chiou, M.C. Maa, C.J. Wang, Mithramycin inhibits human epithelial carcinoma cell proliferation and migration involving downregulation of Eps8 expression, Chem Biol Interact (2009).

[44] M. Sundvall, L. Peri, J.A. Maatta, D. Tvorogov, I. Paatero, M. Savisalo, O. Silvennoinen, Y. Yarden, K. Elenius, Differential nuclear localization and kinase activity of alternative ErbB4 intracellular domains, Oncogene 26 (2007) 6905-6914.

[45] E. Menna, A. Disanza, C. Cagnoli, U. Schenk, G. Gelsomino, E. Frittoli, M. Hertzog, N. Offenhauser, C. Sawallisch, H.J. Kreienkamp, F.B. Gertler, P.P. Di Fiore, G. Scita, M. Matteoli, Eps8 regulates axonal filopodia in hippocampal neurons in response to brain-derived neurotrophic factor (BDNF), PLoS Biol 7 (2009) e1000138.

[46] B. Matoskova, W.T. Wong, A.E. Salcini, P.G. Pelicci, P.P. Di Fiore, Constitutive phosphorylation of eps8 in tumor cell lines: relevance to malignant transformation, Mol Cell Biol 15 (1995) 3805-3812.

[47] R. Gallo, C. Provenzano, R. Carbone, P.P. Di Fiore, L. Castellani, G. Falcone, S. Alema, Regulation of the tyrosine kinase substrate Eps8 expression by growth factors, v-Src and terminal differentiation, Oncogene 15 (1997) 1929-1936.

[48] E.S. Anton, H.T. Ghashghaei, J.L. Weber, C. McCann, T.M. Fischer, I.D. Cheung, M. Gassmann, A. Messing, R. Klein, M.H. Schwab, K.C. Lloyd, C. Lai, Receptor tyrosine kinase ErbB4 modulates neuroblast migration and placement in the adult forebrain, Nat Neurosci 7 (2004) 1319-1328.

[49] G. Sekerkova, M.R. Dino, E. Ilijic, M. Russo, L. Zheng, J.R. Bartles, E. Mugnaini, Postsynaptic enrichment of Eps8 at dendritic shaft synapses of unipolar brush cells in rat cerebellum, Neuroscience 145 (2007) 116-129.